Analytical Solutions and Moments Analysis of Two-Dimensional General Rate Model for Chromatographic Columns of Cylindrical Geometry Considering Dirichlet Boundary Condition

Uche U. D[1], Okechi F. N[2], Uche M[3], and Omoniwa B[4].

[1-3] Mathematics Programme,National Mathematical Centre, Abuja

Email address and phone number:

duj_uche@yahoo.com09055124233,okechinnamdi@hotmail.com08158247454,longsmercy@yahoo.com08037054404.

[4] Corresponding author at National Mathematical Centre Abuja, Department of Computer Science.

Email address and phone number: tunjiomoniwa@yahoo.com07034434646.

Abstract

This work is concerned with the analytical solutions of a two dimensional general rate model simulating liquid chromatographic process in a cylindrical column considering dirichlet boundary condition at the column inlet and outlet. A single-solute model is considered using linear isotherm and pulse injection of finite width at the column inlet. The finite Hankel and Laplace transformations are used simultaneously to solve the model equations. Since the analytical Laplace inversion in the actual time domain is not possible, the numerical inversion is applied. To further analyze the effect of different kinetic parameters on the elution profiles, the first four temporal moments are derived analytically from the solutions in the Laplace domain. These moments can be used to analyze the retention times, band broadenings, front asymmetries and flattening of the elution profiles. The derived solutions will be useful to optimize the process and analyze the effect of involved mass transfer processes.

Key words: General rate model, moments analysis, mass transfer, linear isotherms.

1 Introduction

Liquid chromatography is a separation technique that is used to separate mixture molecules using partitioning characteristics of molecule to remain in a stationary phase in contrast with a mobile phase. Once a molecule is separated from the mixture, it can be isolated and quantified. Such techniques are used in pharmaceutical and chemical engineering industries in a great deal for purification and subsequent analysis. The main ingredients of the liquid chromatography are the mobile and stationary phases. The mobile phase is the solvent entering (eluent) and leaving (eluate) the column, while the stationary phase stays fixed in a place inside the column. The separation is based on the partitioning between the stationary and mobile phases. Different mathematical models exist in the literature describing the chromatographic process. The most notable amongst them are the general rate model (GRM), the equilibrium dispersive model (EDM), and the lumped kinetic model (LKM) [1–3]. All these models need important input information regarding the thermodynamic equilibrium of the distribution of the components between the mobile and stationary phases. They differ essentially regarding the consideration of unavoidable mass transfer processes, which cause undesired band broadening.

The analytical solutions of the two-dimensional advection-dispersion equations (ADE's) in cylindrical coordinates are particularly useful for analyzing problems of the two-dimensional solute transport in a porous medium system with steady uniform flow [4–9].

Analytical solutions and moment analysis of the one-dimensional EDM, LKM and GRM have been derived for linear isotherms using the Laplace transformation [10]. Recently, the analytical solutions and temporal moments of the 2D linear EDM were derived in [11].

In this work, further progress shall be made in this field by solving the 2D linear GRM with several case studies carried out to illustrate the effect of the axial and radial dispersion

coefficients on the effluent concentration profiles.

2 The Model

The chromatographic model is derived from the conservation of massprinciple which

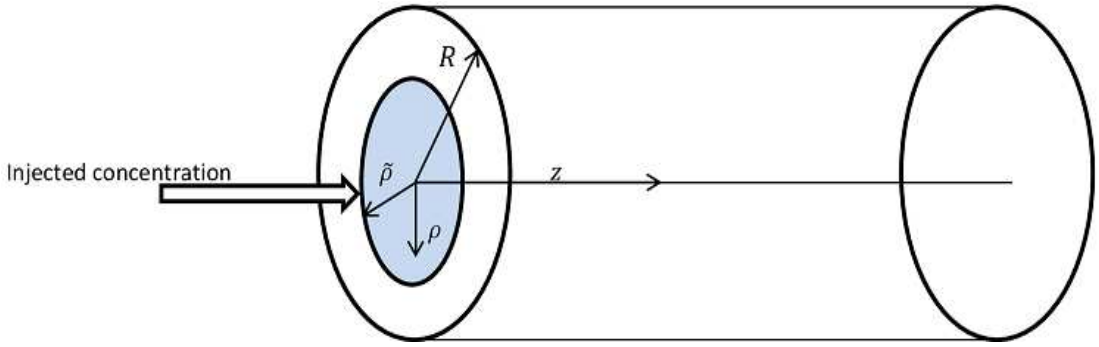

states that the net rate of change of solute masswithin a chromatogram is equal to the

Figure 1: Diagram showing the concentration injection and flow direction in the column of a cylindrical geometry

difference between solute fluxentering and leaving a chromatographic column. This paper deals with the movement of solute in a 2D column ofchromatography in radial geometry as shown in figure 1. The solute injected drifts in the z-direction via axialdispersion and advection, while it transmits in the ρ-directionvia radial dispersion. We unconcern ourselves with the rate of flowchanges and keep the interstitial velocity u as constant in thisstudy. We assume further that the isotherm of adsorption is linear with a Henry constant a. To cause andintensify the reaction of possible rate constraints of the transportof mass in the radial direction, the subsequent particular injectionconditions are made up. We introduce a parameter $\tilde{\rho}$ andthe whole representation of the column is partitioned so as to havean inside spherical core and an exterior circular ring (see figure 1). The injection profile is composed such that it generallyallows for injection either via an inside core, an exterior ring orvia the entire representation. If $\tilde{\rho}$ is set to be thecolumn's radius which is connoted by R, then we have the injectionthrough the whole cross-section.In liquid chromatography, the GRM considers several contributions of the mass transfer processes that lead to band broadening.

In two-dimensional flow, the mass balance equation for a single solute component percolating through a cylindrical column of radius $\tilde{\rho}$ filled with spherical particles of radius R_p, for $i = 1,2,...,N_c$ is given as:

$$\frac{\partial c_i}{\partial t} + u\frac{\partial c_i}{\partial z} = D_{z,i}\frac{\partial^2 c_i}{\partial z^2} - \frac{3}{R_p}Fk_{\text{ext},i}\left(c_i - c_{p,i}(r = R_p)\right) + D_{\rho,i}\left(\frac{\partial^2 c_i}{\partial \rho^2} + \frac{1}{\rho}\frac{\partial c_i}{\partial \rho}\right), \tag{1}$$

In the above equation, c is the concentration of a solute in the bulk phase of the fluid and c_p is the concentration of the same solute in the particle pores. u is the interstitial velocity and D_z is the axial dispersion coefficient. F is the phase ratio and is defined as $F = (1-\varepsilon_b)/\varepsilon_b$, where ε_b is the external porosity. More so, D_ρ represents the radial dispersion coefficient, k_{ext} is the external mass transfer coefficient, N_c denotes the number of components while t and z denote time and axial coordinates of the column respectively. Lastly, r is the radial coordinate of spherical particles of radius R_p and ρ is the cylindrical coordinate of the column of radius $\tilde{\rho}$.

The mass balance equation in the stationary phase for $i = 1,2,...,N_c$:

$$\varepsilon_p\frac{\partial c_{p,i}}{\partial t} + (1-\varepsilon_p)\frac{\partial q^*_{p,i}}{\partial t} = \frac{1}{r^2}\frac{\partial}{\partial r}\left[r^2\left(\varepsilon_p D_{p,i}\frac{\partial c_{p,i}}{\partial r} + (1-\varepsilon_p)D_{s,i}\frac{\partial q^*_{p,i}}{\partial r}\right)\right], \tag{2}$$

Where q^*_p is the local concentration of the solute in stationary phase, D_p is the pore diffusivity, ε_p is the internal porosity and D_s is the surface diffusivity. The frequently applied convex nonlinear Langmuir isotherm can be defined as [12]:

$$q^*_{p,i} = \frac{a_i c_{p,i}}{1 + \sum_{j=1}^{N_c} b_j c_{p,j}}, \qquad i = 1,2,...,N_c \tag{3}$$

But for this case, b_j which is the coefficient of nonlinearity is 0, thus we have the linear isotherm as: $q^*_{p,i} = a_i c_{p,i}$, $i = 1,2,...,N_c$.

In order to reduce the number of variables in the PDE system, the variables are replaced with the following dimensionless parameters:

$$C_i = \frac{c_i}{c_{inj,i}}, C_{p,i} = \frac{c_{p,i}}{c_{\mathrm{pinj},i}}, R = \frac{r}{R_P}, x = \frac{z}{L}, Pe_{zi} = \frac{Lu}{D_{zi}}, Pe_{\rho i} = \frac{\tilde{\rho}^2 u}{D_{\rho i} L},$$

$$\psi = \frac{\rho}{\tilde{\rho}}, \zeta_i = \frac{k_{\mathrm{ext}} R_p}{\varepsilon_p D_{p,i}}, \eta_i = \frac{D_{eff,i} L}{u R_p^2}, \xi_i = 3\zeta_i \eta_i F, \tau = \frac{ut}{L}. \tag{4}$$

Eqs. (1) - (3) is thus transformed by using the dimensionless variables into:

$$\frac{\partial C_i}{\partial \tau} + \frac{\partial C_i}{\partial x} = \frac{1}{Pe_{zi}} \frac{\partial^2 C_i}{\partial x^2} - \xi_i \left(C_i - C_{p,i}(R=1) \right) + \frac{1}{Pe_{\rho i}} \left(\frac{\partial^2 C_i}{\partial \psi^2} + \frac{1}{\psi} \frac{\partial C_i}{\partial \psi} \right) \tag{5}$$

$$\frac{\partial C_{p,i}}{\partial \tau} = \frac{\eta}{\alpha_j R^2} \frac{\partial}{\partial R} \left(R^2 \frac{\partial C_{p,i}}{\partial R} \right), \tag{6}$$

where $\alpha_j = \varepsilon_p \left(1 + \frac{aF}{(1+b_j c_{pj})^2} \right)$.

The following initial and boundary conditions are used for the model:

At $\tau = 0$, the initial conditions are $C_i = C_i(0, x, \psi) = 0$, $C_{p,i} = C_{p,i}(0, x, R, \psi) = 0$.

The above Eqs. (5) and (6), are also subjected to the following corresponding assumed boundary conditions at $\psi = 0$ and $\psi = 1$

$$\frac{\partial C(\psi = 0, x, \tau)}{\partial \psi} = 0, \qquad \frac{\partial C(\psi = 1, x, \tau)}{\partial \psi} = 0. \tag{7}$$

The first and second boundary conditions conforms with the symmetry of the radial profile and the impermeability of the column wall respectively.

$$\frac{\partial C_p(R = 0, \psi = 0, x, \tau)}{\partial \psi} = 0, \qquad \frac{\partial C_p(R = 1, \psi = 1, x, \tau)}{\partial \psi} = \zeta \left(C - C_p \mid_{R=1} \right). \tag{8}$$

Now, at the outlet and the inlet of the column, the following Dirichlet BC is examined:

Finite width concentration pulse injection for Dirichlet inlet boundary

conditions: The boundary condition for inner annular region injection is:

$$C(\psi, x=0, \tau) = \begin{cases} 1, & \text{if } 0 \le \psi \le \tilde{\psi} \text{ and } 0 \le \tau \le \tau_{inj}, \\ 0, & \text{if } \tilde{\psi} < \psi \le 1 \text{ or } \tau > \tau_{inj}. \end{cases} \tag{9}$$

For outer annular zone injection:

$$C(\psi, x=0, \tau) = \begin{cases} 1, & \text{if } \tilde{\psi} < \psi \le 1 \text{ and } 0 \le \tau \le \tau_{inj}, \\ 0, & \text{if } 0 \le \psi \le \tilde{\psi} \text{ or } \tau > \tau_{inj}. \end{cases} \tag{10}$$

and

$$\tilde{\psi} = \tilde{\rho}/R,. \tag{11}$$

Injecting over the entire cross-section inlet of the column, either $\tilde{\psi} = 1$ in (9) or $\tilde{\psi} = 0$ in (10).

Hypothetically of infinite length ($x = \infty$), the following outflow Neumann boundary condition is considered at the outlet of the column:

$$\left.\frac{\partial C_i}{\partial x}\right|_{x=\infty} = 0. \tag{12}$$

The equations of the model, together with the associated initial and boundary condition are solved analytically by first applying the finite Hankel transform and then the Laplace transform. Thus, the Hankel transformation of Eq. (5) with respect to ψ gives

$$\frac{\partial C_H}{\partial \tau} + \frac{\partial C_H}{\partial x} = \frac{1}{Pe_z}\frac{\partial^2 C_H}{\partial x^2} - \xi\left(C_H - (C_p)_H\,|_{R=1}\right) - \frac{\lambda_n^2}{Pe_\rho} C_H. \tag{13}$$

Now using the Laplace transform on Eq.(13) with respect to τ, gives:

$$\frac{1}{Pe_z}\frac{\partial^2 \overline{C}_H}{\partial x^2} - \frac{\partial \overline{C}_H}{\partial x} - \xi\left(\overline{C}_H - \overline{(C_p)}_H\,|_{R=1}\right) - \left(s + \frac{\lambda_n^2}{Pe_\rho}\right)\overline{C}_H = 0. \tag{14}$$

After rephrasing Eq. (6), we obtain:

$$a^* \frac{\partial}{\partial \tau}\left(RC_p\right) - \eta \frac{\partial^2}{\partial R^2}\left(RC_p\right) = 0, \tag{15}$$

with the corresponding boundary conditions:

$$\frac{\partial C_p}{\partial R}|_{R=0} = 0, \quad \frac{\partial C_p}{\partial R}|_{R=1} = \zeta\left(C - C_p\,|_{R=1}\right). \tag{16}$$

Furthermore, applying the Laplace transformation on Eq. (15) gives:

$$\frac{d^2\left(R\overline{C}_p\right)}{dR^2} - \alpha(s) R\overline{C}_p = 0. \tag{17}$$

The general solution of the above equation is given as:

$$\overline{C}_p = \frac{1}{R}\left(Ae^{\sqrt{\alpha(s)}R} + Be^{-\sqrt{\alpha(s)}R}\right), \tag{18}$$

where, $\alpha(s) = \frac{a^* s}{\eta}$. Here, A and B are the constants to be determined using the boundary conditions given in Eq. (16) which gives:

$$A = \frac{\zeta\overline{C}/2\sinh(\sqrt{\alpha(s)})}{(\zeta - 1) + \sqrt{\alpha(s)}\coth(\sqrt{\alpha(s)})}, \tag{19}$$

and

$$B = -\frac{\zeta\overline{C}/2\sinh(\sqrt{\alpha(s)})}{(\zeta - 1) + \sqrt{\alpha(s)}\coth(\sqrt{\alpha(s)})}. \tag{20}$$

Thus, the solution in Eq. (18) at $R = 1$, takes the form

$$\overline{C}_p\,|_{R=1} = \overline{C} f(s), \tag{21}$$

where

$$f(s) = \frac{\zeta}{(\zeta - 1) + \sqrt{\alpha(s)}\coth(\sqrt{\alpha(s)})}. \tag{22}$$

Using the Hankel transform on Eq. (21) with respect to ψ gives:

$$\left(\overline{C}_p\right)_H\,|_{R=1} = \overline{C}_H f(s). \tag{23}$$

Introducing Eq. (23) in Eq. (14), we get the following ordinary differential equation:

$$\frac{d^2\overline{C}_H}{dx^2} - Pe_z \frac{d\overline{C}_H}{dx} - Pe_z \phi(s,\lambda_n)\overline{C}_H = 0, \tag{24}$$

where

$$\phi(s,\lambda_n) = s + \frac{\lambda_n^2}{Pe_\rho} + \xi(1 - f(s)). \tag{25}$$

The solution of this equation is given as

$$\overline{C}_H(\lambda_n, x, \tau) = A_0 e^{m_1 x} + B_0 e^{m_2 x}, \tag{26}$$

where

$$m_{1,2} = \frac{Pe_z}{2}\left(1 \pm \sqrt{1 + \frac{4\phi(s,\lambda_n)}{Pe_z}}\right), \tag{27}$$

and A_0 and B_0 are constants to be determined from the given BCs. The positive sign (upper case) in Eq. (27) is selected for calculating m_1 and the negative sign is used for calculating m_2.

For this to be done, we again consider the following BC at the outlet and inlet of the column: The Hankel-transform of Eqs. (9) [or (10)] and (12) are:

$$C_H(\lambda_n, x = 0, \tau) = \begin{cases} F(\lambda_n), & \text{if } 0 \le \tau \le \tau_{inj}, \\ 0, & \text{if } \tau > \tau_{inj}, \end{cases} \tag{28}$$

$$\left.\frac{\partial C_H(\lambda_n, x, \tau)}{\partial x}\right|_{x=\infty} = 0. \tag{29}$$

For inner cylindrical core injection, $F(\lambda_n)$ is:

$$F(\lambda_n) = \begin{cases} \dfrac{\tilde{\psi}^2}{2}, & \text{if } \lambda_n = 0, \\ \dfrac{\tilde{\psi}}{\lambda_n} J_1(\lambda_n \tilde{\psi}), & \text{if } \lambda_n \neq 0, \end{cases} \tag{30}$$

and for outer annular ring injection, we have it as:

$$F(\lambda_n) = \begin{cases} \left(\frac{1}{2} - \frac{\tilde{\psi}^2}{2}\right), & \text{if } \lambda_n = 0, \\ -\frac{\tilde{\psi}}{\lambda_n} J_1(\lambda_n \tilde{\psi}), & \text{if } \lambda_n \neq 0. \end{cases} \tag{31}$$

Using the Laplace-transform on the BCs in (28) and (29) gives:

$$\overline{C}_H(\lambda_n, x = 0, s) = \frac{F(\lambda_n)}{s}\left(1 - e^{-s\tau_{inj}}\right), \quad \left.\frac{\partial \overline{C}_H}{\partial x}\right|_{x=\infty} = 0. \tag{32}$$

And using Eq. (32) in Eq. (26) gives:

$$A_0 = 0, \qquad B_0 = \frac{\left(1 - e^{-s\tau_{inj}}\right)}{s} F(\lambda_n). \tag{33}$$

Therefore, the solution in Eq. (26) becomes:

$$\overline{C}_H(\lambda_n, x, s) = \frac{\left(1 - e^{-s\tau_{inj}}\right)}{s} F(\lambda_n) e^{m_2 x}, \tag{34}$$

where m_2 is given by (27) for the minus sign.

The Laplace transformation can be used to obtain analytical expressions for the moments because it is a moment generating function. Temporal moments are obtained analytically here as functions of radial coordinate ψ at the exterior of the column ($x = 1$) considering $c_{init} = 0$. The subsequent feature of Laplace-transform was utilized to ascertain the moments analytically from the Hankel and Laplace transformed concentration $\overline{C}_H$ in (34)

$$\mu_{i,H} = (-1)^i \lim_{s \to 0} \frac{d^i(\overline{C}_H(\lambda_n, x, s))}{ds^i}, \quad i = 0,1,2,\cdots. \tag{35}$$

In this paper, the first four moments related to pulse injected rectangular concentration profiles (finite feed volumes) are calculated. It is well known that the first moment μ_1 corresponds to the retention time t_R. The value of the equilibrium constant a can be estimated from the slopes of a straight line, $\mu_1 = t_R$ over $1/u$ for constant column length and porosity. The effects of longitudinal diffusion are not significant with respect to retention

time or first moment. The second moment μ_2, i.e. the variance of the elution profile, provides information about the rates of the mass transfer processes in the column. The third moment μ_3 quantifies the front asymmetries. Lastly, the fourth moment μ_4 measures the kurtosis. Kurtosis determines the peakedness which describes the shape of a probability distribution.

Finite width concentration pulse injection for Dirichlet inlet boundary conditions ((28) and (29)).

Zeroth moment: This is derived for $i = 0$, by defining:

$$w = \sqrt{1 + \frac{4\lambda_n^2}{Pe_z Pe_\rho}}, \tag{36}$$

then we have

$$\mu_{0,H} = \tau_{inj} F(\lambda_n) e^{-Pe_z\left(\frac{w-1}{2}\right)}. \tag{37}$$

Where $F(\lambda_n)$ is expressed by (30) for inner annular region injection and by (31) for outer circular region injection.

First moment: This is obtained for $i = 1$ as:

$$\mu_{1,H} = \left[\frac{\tau_{inj}}{2} + \frac{1 + a^* F}{w}\right]\mu_{0,H}. \tag{38}$$

Second moment: The Second temporal moment is derived for $i = 2$:

$$\mu_{2,H} = \left[\frac{\tau_{inj}^2}{3} + \frac{\left(1 + a^* F\right)}{w}\tau_{inj} + \frac{\left(1 + a^* F\right)^2}{w^2} + \frac{2\left(1 + a^* F\right)^2}{Pe_z w^3}\right.$$

$$\left. + \frac{2a^{*2} F\left(\zeta + 5\right)}{15 w \eta \zeta}\right]\mu_{0,H}. \tag{39}$$

Third moment: For $i = 3$, we get the third temporal moment as:

$$\mu_{3,H} = \left[\frac{\tau_{inj}^3}{4} + \frac{\left(1+a^*F\right)}{w}\tau_{inj}^2 + \left(\frac{3\left(1+a^*F\right)^2}{2w^2} + \frac{a^{*2}F\left(\zeta+5\right)}{5w\zeta\eta} \right.\right.$$

$$\left. + \frac{3\left(1+a^*F\right)^2}{Pe_z w^3}\right)\tau_{inj} + \frac{4a^*F\left(\frac{35}{2}+7\zeta+\zeta^2\right)}{105w\zeta^2\eta^2}$$

$$+ \frac{12\left(1+a^*F\right)^3}{Pe_z^2 w^5} + \frac{4a^{*2}F\left(1+a^*F\right)\left(\zeta+5\right)}{5Pe_z w^3\zeta\eta}$$

$$\left. + \frac{6\left(1+a^*F\right)^3}{Pe_z w^4} + \frac{2a^{*2}F\left(1+a^*F\right)\left(\zeta+5\right)}{5w^2\zeta\eta} + \frac{\left(1+a^*F\right)^3}{w^3}\right]\mu_{0,H}. \tag{40}$$

Fourth moment: For $i = 4$, the fourth temporal moment is given as:

$$\mu_{4,H} = \left[\frac{\tau_{inj}^4}{5} + \frac{\left(1+a^*F\right)}{w}\tau_{inj}^3 + \left(\frac{4\left(1+a^*F\right)^2}{Pe_z w^3} + \frac{4a^{*2}F\left(\zeta+5\right)}{15w\zeta\eta} + \frac{2\left(1+a^*F\right)^2}{w^2}\right)\tau_{inj}^2 \right.$$

$$+ \left(\frac{2\left(1+a^*F\right)^3}{w^3} + \frac{8a^{*2}F\left(1+a^*F\right)\left(\zeta+5\right)}{5Pe_z w^3\zeta\eta} + \frac{8a^{*3}F\left(\frac{35}{2}+7\zeta+\zeta^2\right)}{105w\zeta^2\eta^2} \right.$$

$$\left. \left. + \frac{24\left(1+a^*F\right)^3}{Pe_z^2 w^5} + \frac{12\left(1+a^*F\right)^3}{Pe_z w^4} + \frac{4a^{*2}F\left(1+a^*F\right)\left(\zeta+5\right)}{5w^2\zeta\eta}\right)\tau_{inj} \right.$$

$$+ \frac{32a^{*3}F\left(1+a^*F\right)\left(\frac{35}{2}+7\zeta+\zeta^2\right)}{105Pe_z w^3\zeta^2\eta^2} + \frac{48a^{*2}F\left(1+a^*F\right)^2\left(\zeta+5\right)}{5Pe_z^2 w^5\zeta\eta} + \frac{\left(1+a^*F\right)^4}{w^4}$$

$$+ \frac{8a^{*4}F^2\left(\zeta+5\right)^2}{75Pe_z w^3\zeta^2\eta^2} + \frac{24a^{*2}F\left(1+a^*F\right)^2\left(\zeta+5\right)}{5Pe_z w^4\zeta\eta} + \frac{4a^{*4}F^2\left(\zeta+5\right)^2}{75w^2\zeta^2\eta^2}$$

$$+ \frac{120\left(1+a^*F\right)^4}{Pe_z w^7} + \frac{8a^{*3}F\left(1+a^*F\right)\left(\frac{35}{2}+7\zeta+\zeta^2\right)}{105w^2\zeta^2\eta^2} + \frac{60\left(1+a^*F\right)^4}{Pe_z^2 w^6}$$

$$\left. + \frac{12\left(1+a^*F\right)^4}{Pe_z w^5} + \frac{4a^{*2}F\left(1+a^*F\right)^2\left(\zeta+5\right)}{5w^3\zeta\eta} + \frac{8a^{*4}F\left(175+105\zeta+27\zeta^2\right)}{1575w\zeta^3\eta^3}\right]\mu_{0,H}. \tag{41}$$

3 Results and Discussion

3.1 Linear Isotherms Concentration Profiles

The radius of the inner spherical core $\tilde{\rho}$ has been chosen so as to allow for same area between the inner and outer annular zones. This implies that, for a column of radius $R = 0.2$, the inside annular region radius becomes $\tilde{\rho} = 0.1414$.

Figure 2 shows the result considered for $x = 1$ for which the sample was injected from the inner region at $x = 0$. Furthermore, the transport coefficients were chosen to be $Pe_\rho = 0.5$ and $Pe_z = 20$.

The radial transport in this case is relatively fast and as such, there is no obvious radial concentration dependence over the whole cross section. The next Figure 3 shows the results for average concentration profile for inner and outer annular zones injection. The profiles are identical at $x = 1$ because of the fast expulsion of radial concentration gradients.It is noticeable that Figures 2 and 3 are identical,this is as a result of the fast radial transport.

Figure 4 shows the result for injection through the inner zone, the transport coefficients are given as: $Pe_z = 600$ and $Pe_\rho = 15$. Figure 5 shows the result for injection through the outer zone for the same transport coefficients as in Figure 4. Both results show significant difference as this implies that the transport coefficients affects the profile if injected through the inner or outer zone. Figure 6 shows that the average concentration profiles for the inner and outer zones injection correspond. Significant difference is also noticed between the local and average concentration profiles due to the slower radial transport ($Pe_\rho = 15$).

Figures 7(a–d) shows the effects of mass transfer coefficients (Biot number and η) on the concentration profiles. Also, the results of radial dispersion coefficient on the concentration profiles at the center of the column (that is $x = 0.5$) for $\tau = 1$ are given for both

inner and outer zones injection by Figures 8(a and b). Different values of $Pe_{ratio}\left(\frac{Pe_\rho}{Pe_z}\right)$ were assumed by fixing $Pe_z = 20$ and varying Pe_ρ with the values in the interval $[0.5,5,50]$. The result shows that for greater values of the radial transport coefficients, the step profiles disintegrates very fast. Both cases shows either conservation or expulsion of the injection profiles.

3.2Discussion on the Moments Solution Profiles

The plots of the moments are given in this section, they were plotted to show the effects of the radial and axial coefficients of dispersion on the concentration profile. Figure 9(a) shows that there are no effect of the axial dispersion coefficient on the first moment (which corresponds tothe retention time) as expected. The effects are clearly seen on the second 9(b), as well as on the third 9(c) and fourth 9(d) moments for inner zone injection. Lastly, this section ends with Figures 10 which shows the moments plotted against ρ. Different values of $Pe_{ratio}\left(\frac{Pe_\rho}{Pe_z}\right)$ were assumed also by fixing $Pe_z = 20$ and varying Pe_ρ with the values in the interval $[150,15,1.5]$. The effects of the dispersion coeeficient Pe_ρ can clearly be seen on the profiles.

Table 1: Parameters used for the computer simulation.

Figure number	Dimensionless parameters									
	ε_p	ε_b	Pe_z	Pe_ρ	a	η	Bi	b	C_0	ξ
1,2, 6	0.333	0.4	20	0.5	4	2	50	0	0.1	450
3-6	0.333	0.4	600	15	4	2	50	0	0.1	450

Also, $Pe_{ratio} = \frac{R^2}{L^2}\frac{D_z}{D_\rho} = Pe_\rho / Pe_z$.

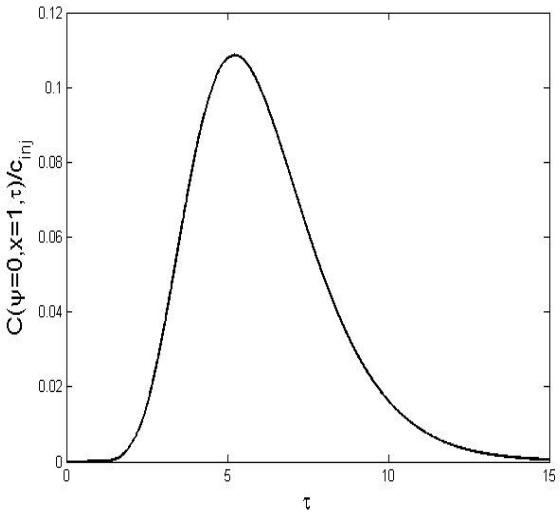

Figure 2: inner zone injection concentration profile for $Pe_\rho = 0.5$ and $Pe_z = 20$

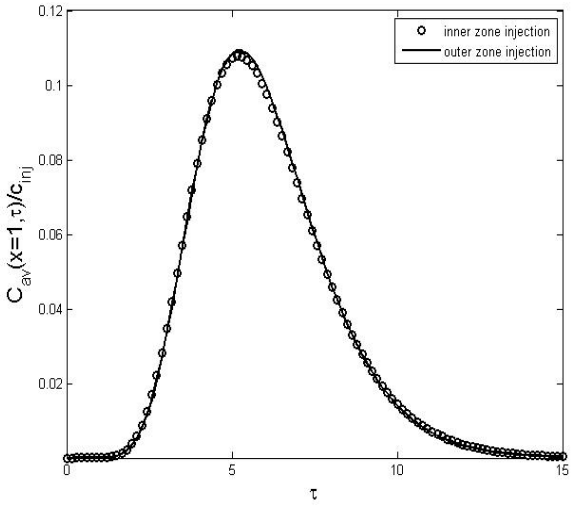

Figure 3: average concentration profile (inner and outer zones injection) for $Pe_\rho = 0.5$ and $Pe_z = 20$

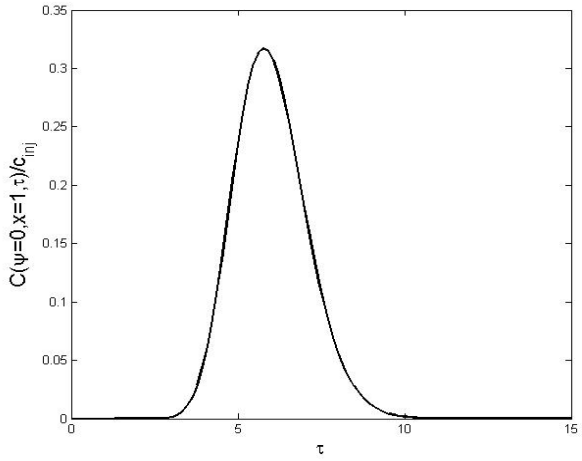

Figure 4: inner zone injection concentration profile for $Pe_\rho = 15$ and $Pe_z = 600$

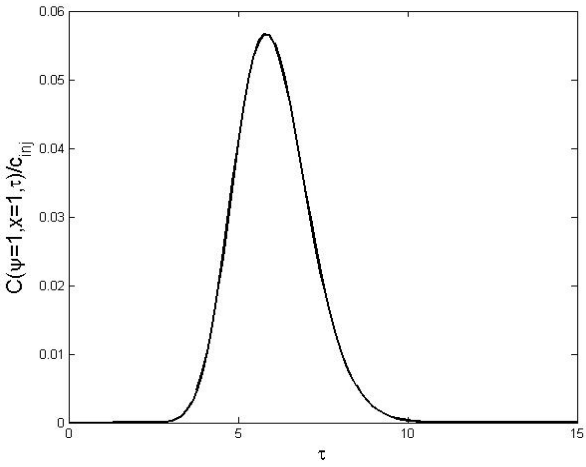

Figure 5: outer zone injection concentration profile for $Pe_\rho = 15$ and $Pe_z = 600$

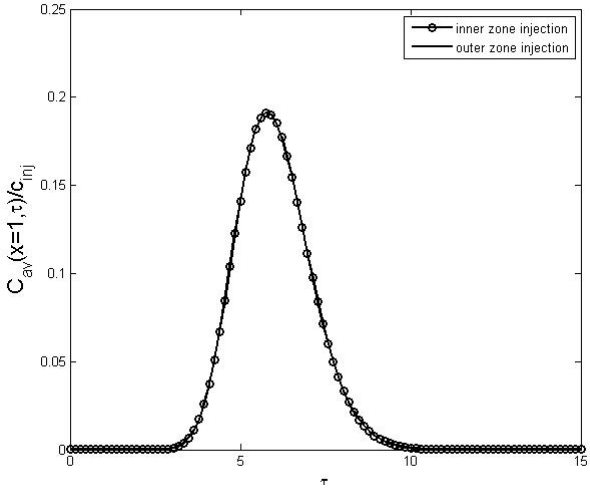

Figure 6: average concentration profile for $Pe_\rho = 15$ and $Pe_z = 600$

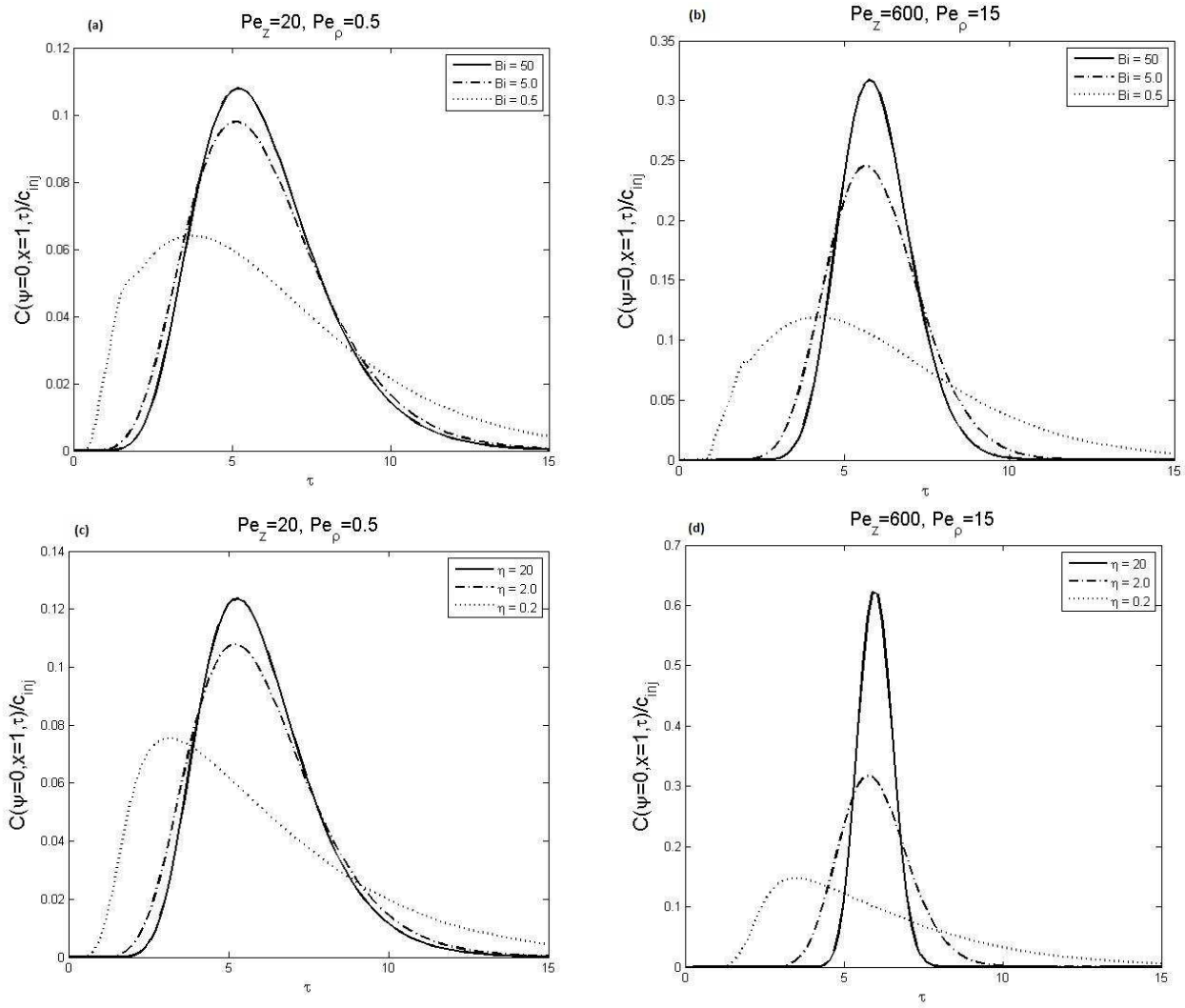

Figures 7: effects of mass transfer coefficients on the concentration profiles

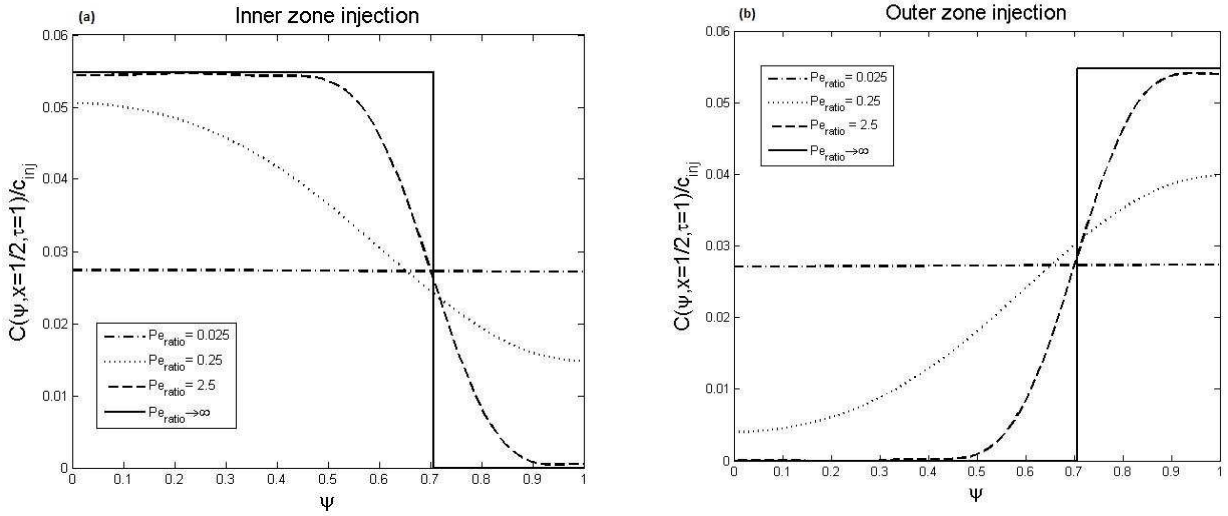

Figures 8: effects of the radial dispersion coefficient on the concentration profile at the centre of the column

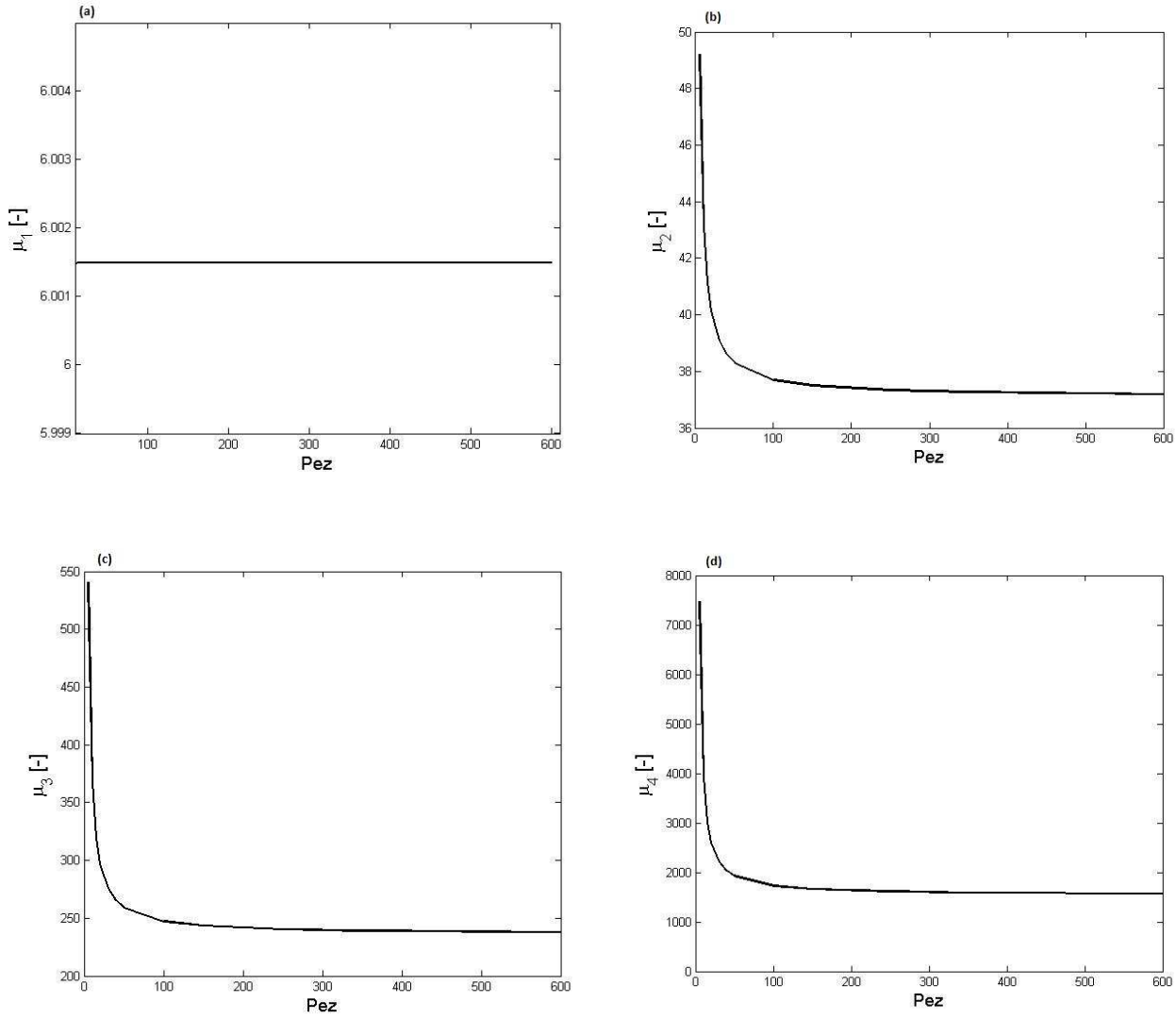

Figures 9: effects of the axial dispersion coefficient on the describing moments

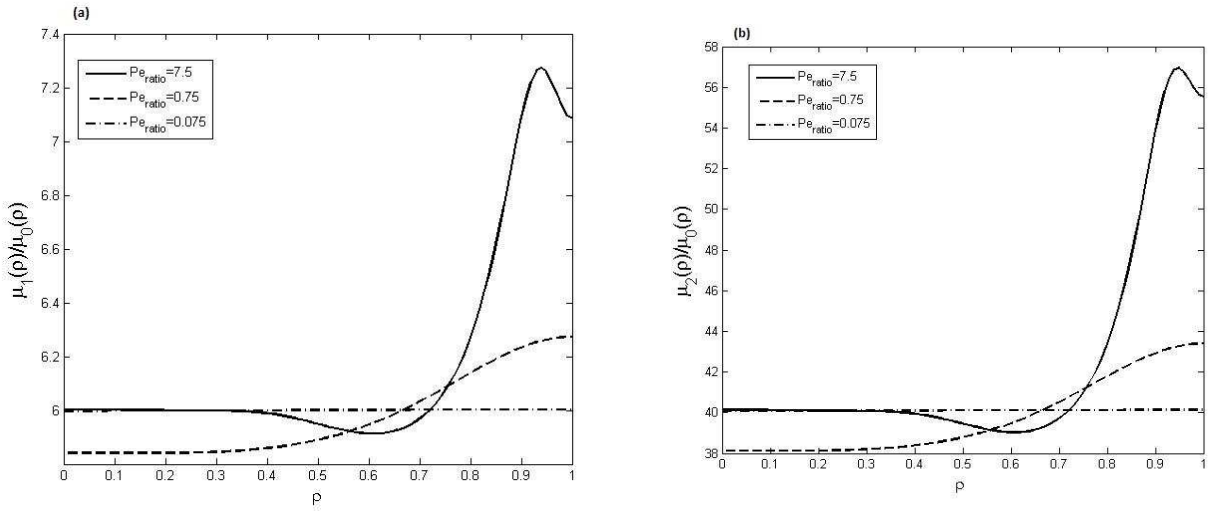

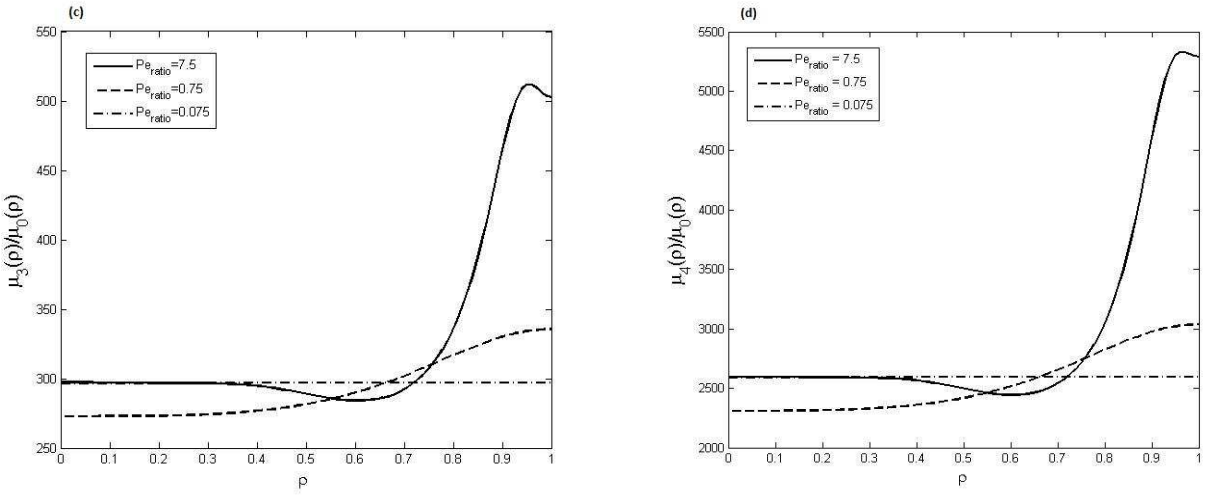

Figures 10: effects of the radial dispersion coefficient on the describing moments

4Conclusion

This study was concerned with the analytical solutions of a two-dimensional GRM for linear isotherms. The Dirichlet boundary condition and pulse injection of finite width was considered. The Hankel and Laplace transformations were applied together to obtain the solutions in the Laplace domain. Afterwards, numerical Laplace inversion was used to get the concentration profiles in the actual time domain. The Laplace domain solutions were used to derive expressions for the first four temporal moments analytically. These moment expression are very useful to describe the effects of different mass transfer processes and to estimate kinetic parameters from the experimental data. The derived solutions could be useful to optimize the separation process.

LIST OF NOTATIONS

a	Henry's constant (Linear adsorption constant) [-]
Bi	Biot number [-]
C_0	maximum concentration of a solute, [g/l]
c	liquid phase concentration, [g/l]
C	dimensionless liquid phase concentration, [g/l]
c_p	concentration in the particle pores, [g/l]
C_p	dimensionless concentration in the particle pores, [g/l]
$\bar{c}$	Laplace transformed concentration, [g/l]
c_{av}	averaged concentration, [g/l]
c_H	Hankel transformed concentration, [g/l]
c_{init}	initial concentration, [g/l]
c_{inj}	injected concentration, [g/l]
D_ρ	radial dispersion coefficient [cm^2/min]
D_p	pore diffusivity [cm^2/min]
D_s	surface diffusivity [cm^2/min]
D_{eff}	effective diffusion coefficient [cm^2/min]
D_z	axial dispersion coefficient [cm^2/min]
k_{ext}	external transfer coefficient, [$1/min$]
Pe_ρ	radial Peclet number, [-]
Pe_z	axial Peclet number, [-]
ρ	radial coordinate of spherical particle of radius R_p, [cm]

References

[1] Guiochon, G., 2002. J. Chromatogr. A, 965, 129-161. Preparative liquid chromatography.

[2] Javeed, S., Qamar, S., Ashraf, W., Seidel-Morgenstern, A., Warnecke, G., 2013. Chem. Eng. Sci. 90, 17-31.Analysis and numerical investigation of two dynamic models for liquid chromatography.

[3] Qamar, S., Abbasi, J.N., Javeed, S., Shah, M., Khan, F.U., Seidel-Morgenstern, A., 2013. J. Chromatogr. A 1315, 92-106.Analytical solutions and moment analysis of chromatographic models for rectangular pulse injections.

[4] Chen, J.-S., Liu, Y.-H., Liang, C.-P., Liu, C.-W., Lin, C.-W., 2011. Adv. Water Resour. 34, 365-374.Exact analytical solutions for two-dimensional advection–dispersion equation in cylindrical coordinates subject to third-type inlet boundary conditions.

[5] Chen, J.-S., Liu, Y.-H., Liang, C.-P., Liu, C.-W., Lin, C.-W., 2011. J. Hydrol. 405, 522-531.Analytical solutions to two-dimensional advection–dispersion equation in cylindrical coordinates in finite domain subject to first- and third-type inlet boundary conditions.

[6] Massabó, M., Cianci, R., Paladino, O., 2006. Environ. Modell. Softw. 21, 681–8.

Some analytical solutions for two-dimensional convection–dispersion equation in cylindrical geometry.

[7] Massabò, M., Catania, F., Paladino, O., 2011. Adv. Water Resour. 34, 365–374.Exact analytical solutions for two-dimensional advection–dispersion equation in cylindrical coordinates subject to third-type inlet boundary condition.

[8] Park, E., Zhan, H., 2001.J. Contam. Hydrol. 53, 41-61. Analytical solutions of contaminant transport from finite one-, two, three-dimensional sources in a finite-thickness aquifer.

[9] Zhang, X., Qi, X., Zhou, X., Pang, H., 2006. J. Hydrol. 328, 614-619.

An in situ method to measure the longitudinal and transverse dispersion coefficients of solute transport in soil.

[10] Qamar, S., Abbasi, J.N., Javeed, S., Seidel-Morgenstern, A., 2014.Chem. Eng. Sci. 107, 192-205. Analytical solutions and moment analysis of general rate model for linear liquid chromatography.

[11] Qamar, S., Khan, F.U., Mehmood, Y., Seidel-Morgenstern, A., 2014.Chem. Eng. Sci. 116, 576-589. Analytical solution of a two-dimensional model of liquid chromatography including moment analysis.

[12] Guiochon, G., Felinger, A., Shirazi, D.G., Katti, A.M., 2006. 2nd ed. ELsevier Academic press, New York.Fundamentals of preparative and nonlinear chromatography.